PII: S0032-3861(96)00632-5

Polymer Vol. 38 No. 6, pp. 1303–1315, 1997

0032-3861/97/$17.00+0.00

Temperature, strain rate, and strain state dependence of the evolution in mechanical behaviour and structure of poly(ethylene terephthalate) with finite strain deformation

J. S. Zaroulis and M. C. Boyce*
Department of Mechanical Engineering, Massachusetts Institute of Technology, Cambridge, MA 02139, USA
(Received 28 December 1995; revised 21 May 1996)

Mechanical tests and differential scanning calorimetry (d.s.c.) analysis that characterize the effects of temperature, strain rate and strain state on the finite deformation and occurrence of strain-induced crystallization of initially nearly amorphous poly(ethylene terephthalate) (PET) are presented. Uniaxial compression in the glassy (25–60°C) and glass transition (T_g) regime (60–76°C), over a wide range of strain rates (0.005–0.5 s^{-1}), shows a decrease in the yield stress and flow stress and a small decrease in the strain hardening modulus, with an increase in temperature and a decrease in strain rate. Post-deformation thermograms on specimens deformed to an imparted logarithmic strain of −1.5 show a decrease in the cold crystallization temperature with an increase in deformation temperature and imparted strain and no change in the cold crystallization exotherm and crystallinity from their pre-deformation values. It follows that uniaxial compression below and through the T_g region induces network orientation without strain-induced crystallization (SIC). However, uniaxial compression in the rubbery regime at 80°C, 0.5 s^{-1} and imparted logarithmic strains up to − 1.75 show a distinctively larger strain hardening from that observed at 0.005 s^{-1}. D.s.c. analysis on the specimens deformed at the rapid rate condition shows that the different strain hardening behaviour may be the result of SIC. The plane strain deformation in the glassy and T_g regions is characterized by an apparent increase in the yield stress and a larger strain hardening behaviour than that observed in uniaxial compression. D.s.c. analysis on the plane strain specimens shows the evolution of both molecular orientation and crystallization at all temperatures which are expected to contribute to the strain hardening. As the temperature in the transition region, it is not clear how much of the end crystallinity, of the order of 41%, is the result of SIC during straining or annealing of the stretched PET after deformation as it cools from the test temperature.

(Keywords: poly(ethylene terephthalate); deformation; temperature dependence; strain-induced crystallization; strain hardening)

INTRODUCTION

Poly(ethylene terephthalate) (PET) is a thermoplastic material found in numerous commercial applications in the form of films of different thickness, crystallinity and orientation. It is used frequently in photographic films, electrical applications (high quality electrical insulation cable wraps) and food packaging. The primary modes of PET processing are blow moulding, vacuum forming, drawing, and biaxial stretching. During these processing modes, the polymer can take either an oriented amorphous or semicrystalline structural state. It thus exhibits the ability to undergo crystallization during processing; a phenomenon that is often termed strain or stress-induced crystallization. The occurrence of strain-induced crystallization provides increased stiffness and hardness as well as better dimensional stability or resistance to recovery.

Hence, the processing of PET near, in, or slightly above its glass transition temperature (T_g) combined with its ability to crystallize during straining makes this material not only commercially viable but also of significant interest to the polymer scientist and mechanical engineer. Of particular interest is the determination of the contribution of molecular orientation vs that of strain-induced crystallization to the hardening of PET with deformation. PET has been the subject of numerous investigations over the past thirty years, some of which will be reviewed below. In the work of this paper we will present our recent research into the three dimensional rate and temperature dependent large strain deformation behaviour of PET. Experiments will be presented which sample the behaviour of the material under different states of large strain and over a wide range of temperature spanning the glassy, the glass transition and the rubbery regime. The differential scanning calorimetry method (d.s.c.) is then used to determine the crystallinity content as a function of the mechanical loading (strain state, magnitude of imposed strain, temperature of the imposed strain). D.s.c. together with the mechanical tests permit the assessment of any potential contribution of crystallization to the strain hardening process.

* To whom correspondence should be addressed

EXPERIMENTAL

Background

Research on the mechanical behaviour of PET starts, for example, with the early work of Marshall and Thompson[1,2], Thompson[3] and Ward[4], and extends to current research, e.g. refs 5–11. A variety of experimental and analytical investigations, only a few of which are mentioned here, have examined the effects of temperature, deformation rate, state of deformation, material anisotropy and heat transfer on the elastic, plastic and finite deformation behaviour of PET.

Early work by Marshall and Thompson[1] on the continuous, heated drawing of initially amorphous PET examined the sensitivity of necking and the corresponding natural draw ratio (NDR) to deformation temperature (20–80°C) and draw speed (5–70 cm s^{-1}). It was shown that NDR increases with decreasing temperature and increasing speed. In other work at deformation temperatures above T_g (i.e. 100°C), Thompson[3] studied the stress-extension curves produced in roller drawing. It was found that rapid draw speed deformations result in large strain hardening of the material at extensions of the order of 300%. Subsequent X-ray analysis revealed high crystallinity in the drawn fibres; hence, strain hardening was attributed to the development of strain-induced crystallization. Ward[4] examined the cold drawing of PET at room temperature over a range of deformation conditions and for different polymer constitutions, i.e. different values of cross-linking, pre-orientation and initial crystallinity content. Birefringence and moduli of cold drawn fibres were fitted by a simple model which assumed that the drawn fibre consists of an aggregate of mechanically anisotropic units that were aligned by the drawing process. Also determination of the natural draw ratios and shrinkages of slightly pre-oriented fibres showed that the natural draw ratio could be regarded as equivalent to a network stretched to its limiting extension. In other work, Ward *et al.*[12] collected data over a variety of temperatures and rates in order to examine its pressure sensitivity.

In other work on strain-induced crystallization, Misra *et al.*[8] investigated the microstructure of PET films stretched both below and above T_g using small angle light scattering (SALS), optical microscopy and wide angle X-ray scattering (WAXS). Annealing the necked portions of the samples that were stretched to 200% below T_g (25°C) resulted in considerable crystallinity. For the samples tested above T_g and subsequently quenched to 0°C, crystallinity was found to increase considerably after a strain of 0.8 at a test temperature of 80°C and a strain rate of 300% min^{-1}. In relatively recent work, Jabarin and Chandran[13,14] have investigated extensively the strain-induced crystallization phenomenon in the rubbery region through the simultaneous and sequential bi-axial stretching* of initially amorphous films at temperatures above T_g (80–105°C) and strain rates that range from 5 to 200% s^{-1} up to limiting extension ratios of 4. It was shown that under these conditions PET undergoes strain-induced crystallization. The crystallization is manifested as a pronounced increase in strain hardening that commences at a temperature and strain rate dependent level of strain, termed the strain hardening parameter. When deformation is slow, however, strain-induced crystallization does not occur since relaxation phenomena dominate over orientation phenomena and the strain hardening modulus is low. The crystalline content of the deformed specimens are assessed from density measurements and the orientation from birefringence; both consistently show the structural evolution of PET from amorphous to semicrystalline with finite strain deformation.

Porter and coworkers[5–7] have conducted extensive tests on the deformation of PET and poly(ethylene-2,6-naphthalate) (PEN) and subsequently have investigated the effects of extent of deformation and deformation temperature on the material microstructure. More specifically, Ghanem and Porter[5] performed isothermal solid state coextrusion tests on isotropic amorphous PEN below and above its T_g and subsequently studied the behaviour of the cold crystallization temperature (T_{cc}) with extrusion temperature and draw ratio. Their d.s.c. analysis revealed that T_{cc} decreases markedly with increasing draw ratio and goes through a minimum in the vicinity of the glass transition region. Also, strain-induced crystallization was found to increase with draw ratio and draw temperature to a saturation value. Guan *et al.*[6] studied the planar deformation of PET in equal biaxial stretching and forging at temperatures above T_g, i.e. 80–110°C, and monitored the structural evolution of PET with d.s.c. WAXS density and recovery measurements. They observed that, as the biaxial draw ratio increases at 90°C, the area of the cold crystallization exotherm decreases, thus manifesting the presence of strain-induced crystallization upon large deformations. Their tests also demonstrated that thermal relaxation processes become more pronounced as the deformation temperature increases away from T_g, therefore, hindering crystallization. Sun *et al.*[7] conducted solid state coextrusion on initially amorphous PET below T_g, 50–70°C, at various draw ratios and subsequently evaluated the cold crystallization behaviour of the co-extrudates. They found that T_{cc} decreases with extrusion draw ratio and also that for extrusion draw ratios up to 2.5†, T_{cc} decreases with extrusion temperature whereas above that value the trend is reversed. Finally, Buckley *et al.*[9] have recently conducted deformation tests on initially amorphous PET under conditions of biaxial stress at elongation rates ranging between 1 and 32 s^{-1} and temperatures ranging between 75 and 120°C. They found the yield stress to decrease with increasing temperature and/or decreasing elongation rate and large strain hardening to initiate at nominal strains of the order of 1.5. Density measurements that were performed on biaxially deformed samples showed that crystallinity increases with maximum principal strain.

It is evident from the above review that a comprehensive set of mechanical tests with subsequent microstructural analysis on the deformed material can provide a picture of the structural evolution of PET; increasing the extent of deformation acts to orient the macromolecular network that under favourable conditions such as high temperature and rapid deformation rate, leads to strain-induced crystallization. The current work examines the mechanical behaviour of initially amorphous PET in the glassy and

* The stretch state that is induced in the material from the simultaneous biaxial extension is very similar to that induced from the uniaxial compression mode

† A tensile draw ratio of 2.5 is analogous to a tensile logarithmic strain of 0.92

glass transition regions where the effects of thermal ageing and the relative importance of configurational to intermolecular energy barriers to deformation are still not well understood nor are they well modelled. It also moves further in the rubbery region in the attempt to characterize strain-induced crystallization phenomena. The experimental part of the investigation, i.e. mechanical tests and microstructural analysis, is presented in detail in this paper.

Material/specimen description

The material that was used in our experiments is amorphous isotropic PET supplied in sheet form from ICI films, UK; the average thickness of the sheet is 1.73 mm. The material appears optically clear, thus implying a very low crystallinity content; d.s.c. measurements revealed a residual crystallinity of the order of 9%*. The small amount of residual crystallinity is a result of the practical difficulties encountered in quenching the polymer rapidly from the melt, i.e. controlling the film thickness, the temperature of the cooling drum, etc. in the effort to obtain an initially amorphous material. Birefringence measurements on similarly prepared ICI film indicate a high degree of isotropy[9] for the received film. Uniaxial and plane strain compression tests were conducted in order to explore the material behaviour. Typically (see, for example, Arruda and Boyce[15,16]), in compression testing, a specimen height to diameter ratio of close to unity is used in order to avoid potential buckling and/or shearing of the specimen; additionally, a lubricant such as thin teflon film is placed between the compression platens and the specimen in order to eliminate friction and the specimen barrelling associated with friction. These geometric ratios together with the lubricant and concentricity of loading act to provide homogeneous deformation of the specimen to very large strains. In the current work, the sheet thickness is only 1.73 mm which poses the problem of specimen size and aspect ratio, especially when considering that the material will be compressed to a true compressive strain of -1.75, therefore, causing a height reduction of the order of 85%.

Trial experiments on commercially available bulk polycarbonate (PC) guided the compression specimen design for the PET sheet. Room temperature uniaxial compression tests at a strain rate of $0.001\,s^{-1}$ were conducted with PC samples of variable height to diameter ratio. It was found that samples with an initial height to diameter ratio in the range of 0.4–1.1 provided identical and repeatable stress vs strain results indicating little influence of sample size and/or friction on the measurement thus providing a sound basis for subsequent material testing. Therefore, an initial height to diameter ratio of 0.45 was chosen for the PET sheet. Each specimen consisted of a stack of three disks with a disk diameter of 12.7 mm. A photograph of an undeformed and one deformed (to a logarithmic strain of -1.5) specimen is shown in *Figure 1*.

A similar rationale was used to produce specimens for the plane strain compression tests: Rectangular pieces of width $w = 9.53$ mm and length $l = 8.64$ mm were cut; a stack of three was used to construct a specimen. The specimen geometries and corresponding test conditions were found to give nearly homogeneous deformations to a final (uniaxial and plane strain) true strain of -1.3[†].

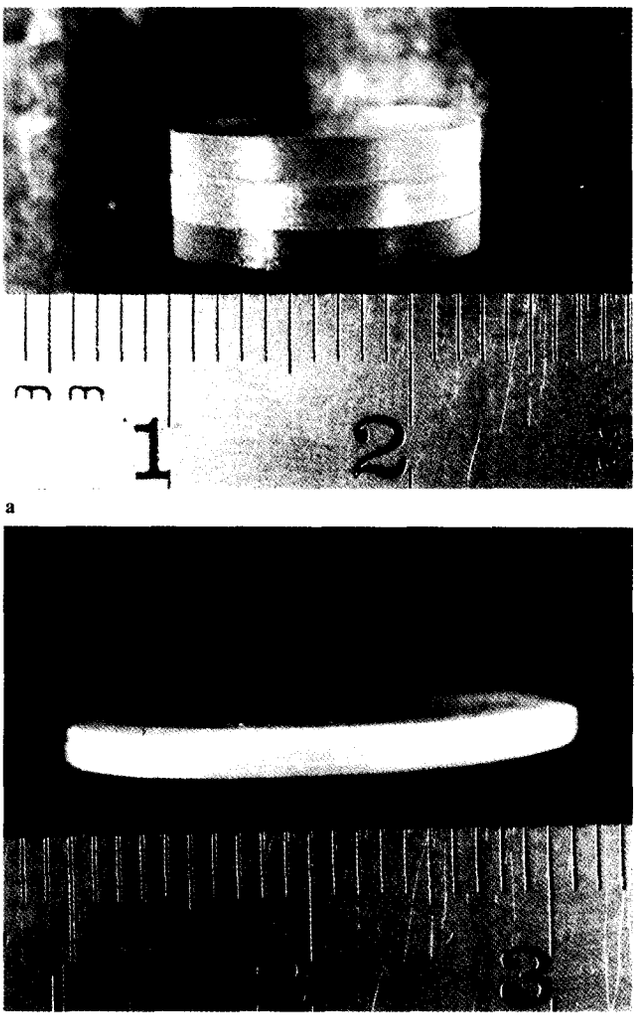

Figure 1 Uniaxial compression specimens undeformed (a), deformed to an imposed strain of -1.5 (b)

Description of mechanical tests

Uniaxial and plane strain compression tests over a range of strain rates and temperatures were conducted in order to measure the stress vs strain behaviour of PET as a function of strain state, strain rate and temperature. The temperature range spans from 25 to 80°C where the T_g is approximately 73.5°C[‡]. The strain rate range spans from the slow isothermal rate of $-0.005\,s^{-1}$ to a fast adiabatic rate of $-0.5\,s^{-1}$. Compression modes were chosen over the tensile mode, since at some temperatures tension typically results in inhomogeneous deformations at finite strains (i.e. necking). Also a uniform specimen temperature is more easily maintained in compression tests than in tensile stretching experiments and therefore

* Crystallinity was estimated from d.s.c. analysis. From the measured enthalpies of cold crystallization and melting and a heat of fusion for PET crystals equal to $120\,kJ\,kg^{-1}$, the crystallinity content was estimated assuming a two phase model

† Some inhomogeneous deformation occurred at the ends of the plane strain specimen due to the one layer locally rolling over the other layer. This end effect did not affect consistency or repeatability of stress vs strain results prior to strains of -1.3; some effects were observed from strains of -1.3 to -1.5.

‡ As measured from d.s.c. analysis at $10°C\,min^{-1}$

Table 1 Comparison of unsteady conduction time to experimental time

Strain rate (s^{-1})	−0.005	−0.01	−0.1	−0.5
t_{exp}(s)	300	150	15	3.0
t_{cond}(s)	10.349	10.349	10.349	10.349
t_{exp}	28.98	14.49	1.449	0.289
Heat transfer condition	isothermal	isothermal	coupled	adiabatic

permits a more accurate assessment of the temperature sensitivity of the mechanical behaviour. This is particularly important when attempting to obtain mechanical data over temperature ranges where the material behaviour varies markedly with a small (say, 2°C) change in temperature. Therefore, a set of compression experiments provides excellent conditions for examining the inherent material constitutive behaviour as a function of temperature and strain rate.

The mechanical tests were performed on an Instron 1350 servohydraulic machine using a Macintosh for control and real time data acquisition via a Keithley 550 D/A and A/D interface. The tests were performed in the strain control mode with a 2620-824 extensometer in order to eliminate the Instron load train compliance errors. During experimental time, strain (a logarithmic strain measure is used) was monitored as a function of time and fed back to the controller in order to alter the actuator displacement rate to provide constant strain rate conditions during the entire deformation. For the elevated temperature tests, a radiant furnace was used to bring the sample to the desired experimental temperature. The time required for the environment of the furnace to reach thermal equilibrium was between 20 and 30 min*. The sensitivity of the mechanical properties of the material at test temperatures near T_g motivated a careful temperature control for the mechanical tests. In the uniaxial compression mode, the specimen temperature was monitored prior to and during the course of the experiment with three type-K thermocouples that were positioned in different positions on the sample circumference and extra thermocouples welded on the stationary (top) compression platen of the Instron. In the plane strain compression mode, thermocouples were welded on the plane strain fixture and some were positioned in the fixture in contact with the specimen. This method allowed us to obtain consistent results over a wide range of temperatures. For further details on our experimental procedure the reader is referred to refs 15 and 18–20.

Due to the range of the strain rates, the duration of the tests varied from approximately 3 s for the $-0.5\,s^{-1}$ rate to 300 s for the $-0.005\,s^{-1}$ rate. We note that the inelastic nature of the deformation results in heat dissipation which may or may not produce a temperature rise in the specimen during the test depending on the strain rate and the experimental temperature of the test. It should be apparent that the faster the rate, the less time for heat transfer, hence the more important the adiabatic effects. Also the higher the experimental temperature, the smaller is the value of the plastic work input to the sample and hence the lower the temperature rise under heating conditions. We classify a test as isothermal, thermomechanically coupled or adiabatic by comparing the duration of the loading cycle, t_{exp} to the time required for heat to transfer out of the specimen t_{cond}, with the following first order analysis. If h_i is the instantaneous height of the sample and the dominant mode of heat transfer in the course of the experiment is conduction of heat from the uniaxially compressed sample to the compression platens, then, the characteristic length that controls the heat transfer is the distance from the platen to the centre of the sample; namely half the current sample height, h_i. It follows that the time required for heat to escape the sample t_{cond} is given as

$$t_{cond} = \frac{(h_i/2)^2}{2k/\rho c} \tag{1}$$

where $k = 0.218\,W\,mK^{-1}$, is the thermal conductivity, $\rho = 1330\,g\,cm^{-3}$, is the density of amorphous PET and, $c = 1300\,J\,kg\,K^{-1}$, is the specific heat capacity†. For a constant strain rate test the loading time required to reach the strain t_{exp} is given by the ratio of the imparted strain $\epsilon_{\perp} = -1.5$ to the strain rate $\dot{\epsilon}$. The calculations presented in *Table 1* show that the experimental time is much shorter than the heat transfer time for the $-0.5\,s^{-1}$ rate, hence, the heat transfer conditions during the latter rate are expected to be adiabatic.

The same first order analysis can be applied for the plane strain compression tests that were performed at the $-0.01\,s^{-1}$ rate. Calculations show the test to be isothermal.

Description of d.s.c. measurements

D.s.c. monitors the rate of change of enthalpy of the material as a function of increasing temperature at a given heating rate. Information on the microstructure and internal energy content of the material can be obtained from the d.s.c. scan through proper data reduction and interpretation. We note that aspects of the d.s.c. scan, e.g. the exact location of the Tg, are somewhat dependent on the imposed heating rate and that the kinetic effects cannot be eliminated from the d.s.c. readings. Therefore, care must be taken in choosing a heating rate and only thermograms with the same rate should be compared with one another when interpreting the enthalpy content in the polymer. Furthermore, a compromise should always be sought between a fast rate that would cause non-uniform heating of the sample and a very slow rate that could cause ageing of the sample in the d.s.c. pan. For that purpose our work was performed at a rate of $10°C\,min^{-1}$ and with sample weights ranging from 10 to 20 mg. This is a set of experimental conditions that have been shown to give repeatable results and is typical for polymer samples[22]. All d.s.c. measurements were performed on a Perkin-Elmer DSC-7A with ice as the cooling medium. The instrument was initially calibrated with two known calibrants, zinc and indium. A baseline run was then conducted at the same heating rate in order to measure the residual enthalpy rate between the reference and sample pans. The baseline was subtracted from the subsequent thermograms of the polymer samples during real time. D.s.c. thermograms were taken on the as-received material as well as on

* According to Imai *et al.*[17], the induction period for crystallization of melt quenched PET due to annealing at 80°C is ≈ 100 min. Having annealed our samples in the thermal environment of the furnace for much shorter times and at lower temperatures we argue that we have not crystallized our samples prior to testing. This was verified using d.s.c.

† Property values extracted from the Polymer Handbook[21]

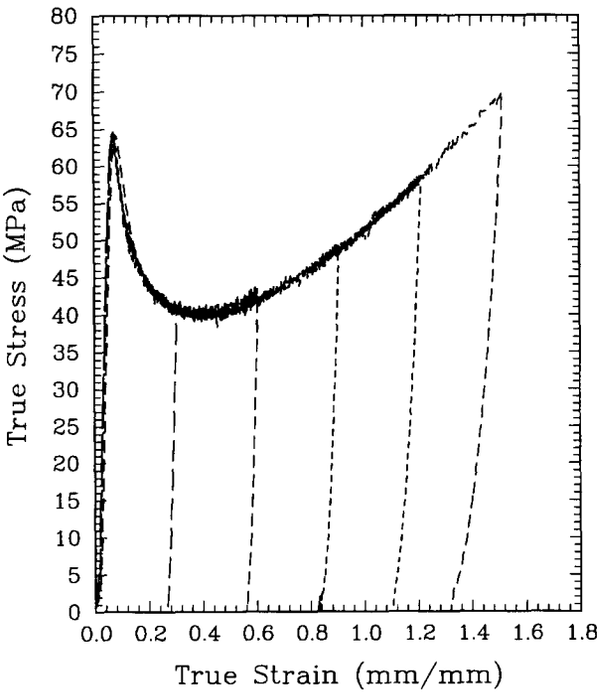

Figure 2 Isothermal uniaxial compression at 25°C, 0.01 s^{-1}, and different levels of strain

samples deformed* at different temperatures, strain rates, strain states and to different final strains in order to assess the effects of deformation conditions on crystallization.

EXPERIMENTAL RESULTS

In this section, results from the mechanical tests and the d.s.c. measurements are presented. Effects of temperature, strain rate and imparted strain are discussed separately for the mechanical tests. The d.s.c. discussion presents the cold crystallization phenomena and its use in assessing strain-induced crystallization.

Mechanical tests

Uniaxial compression and plane strain compression tests were conducted from 25 to 80°C and strain rates of −0.005, −0.01, −0.1 and −0.5 s^{-1}. The results of the tests are presented in terms of true stress vs true strain. The true strain ϵ, is defined as the natural logarithm of the current height, h, to the initial height h_o, namely, $\epsilon = \ln(h/h_o)$. The true stress is the ratio of the current force F to the current area A, namely $\sigma = F/A$, where the current area is computed using the measured current height and assuming incompressibility of inelastic deformation.

Figure 2 shows a set of isothermal uniaxial compression loading–unloading curves at a temperature of 25°C, strain rate of −0.01 s^{-1}, to final strains of −0.3, −0.6, −0.9, −1.2 and −1.5 respectively. Initially, the deformation is linear elastic with the stress increasing proportionally with strain. There is then a nonlinear region prior to yield followed by yield, where the stress reaches a maximum with a corresponding yield strain of approximately −0.07. After yield, the stress is observed to decrease with increasing strain (i.e. strain soften) to a minimum which we term the flow stress. This is the strain softening phenomenon also observed in poly(methyl methacrylate) (PMMA), polystyrene (PS), and PC, for example, by Arruda and Boyce[15] and then Hasan and Boyce[23]. After strain softening, a monotonic increase in the true stress with true strain is observed and the material is said to strain harden. The strain hardening is observed to be nonlinear with the hardening slope increasing with strain. The unloading profiles of the tests show that during unloading the material initially behaves in a linear elastic manner followed by nonlinear recovery. The degree of nonlinear recovery increases with increasing strain and some additional recovery occurs after unloading. The amount of additional recovery is shown in *Table 2* where, for each test shown in *Figure 1*, the imparted strain, final strain after unloading and measured residual strain after 48 h are reported. The residual strain is a manifestation of plastic deformation locked in the material at that particular deformation temperature.

Table 2 Imparted strain, residual strain immediately after unloading and residual strain after 48 h for the uniaxial compression at 25°C and −0.01 s^{-1}

Imparted strain	Res. strain after unloading	Res. strain after 48 h
0.3	0.26	0.20
0.6	0.55	0.45
0.9	0.83	0.72
1.2	1.1	0.96
1.5	1.32	1.17

Below, the effects of temperature, strain rate and strain state on the distinctive features of the mechanical behaviour, elasticity, onset of plastic deformation, strain softening, strain hardening are examined.

Effects of deformation temperature. *Figure 3* shows the isothermal uniaxial compression in the glassy region at 25, 50 and 60°C at a strain rate of −0.01 s^{-1}, thus, demonstrating the effect of temperature in the glassy region. It is evident, that as the temperature increases, the elastic modulus, yield stress and flow stress decrease. Strain softening† is insensitive to temperature and occurs over the same level of true strain for all three temperatures. Subsequent to strain softening, strain hardening decreases moderately with temperature.

Figures 4 and *5* show the isothermal uniaxial compression in the glass transition region over the temperature range 60–76°C at strain rates of −0.01 s^{-1} and −0.1 s^{-1} thus demonstrating the effects of deformation temperature on the mechanical behaviour in that region. From the two figures it is observed that:

1. As the deformation temperature increases, the elastic compressive modulus‡ decreases monotonically with temperature.
2. As the deformation temperature increases, the yield stress and flow stress decrease. However, the yield stress

* D.s.c. specimens were cut carefully from the deformed sample centres, with the help of a Buehler Isomet low speed saw, in order to eliminate any end effect phenomena from the compression tests on the subsequent d.s.c. readings

† Decrease in the difference between the yield stress and the flow stress with strain

‡ The elastic modulus was measured as the steepest slope of the stress strain curve at each experimental condition. Comparison of companion dynamic mechanical analysis (d.m.a.) modulus measurements with the above method were found in reasonable agreement

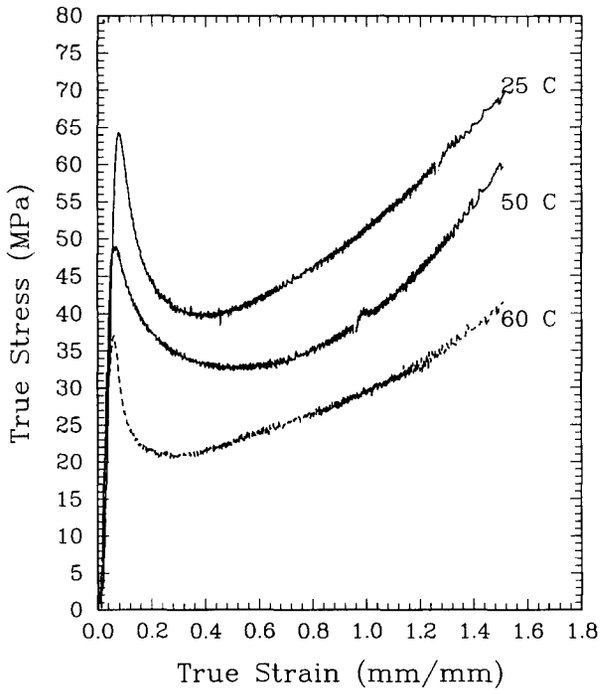

Figure 3 Isothermal uniaxial compression at 25, 50, 60°C and $-0.01\,s^{-1}$: effect of deformation temperature on mechanical properties in the glassy region

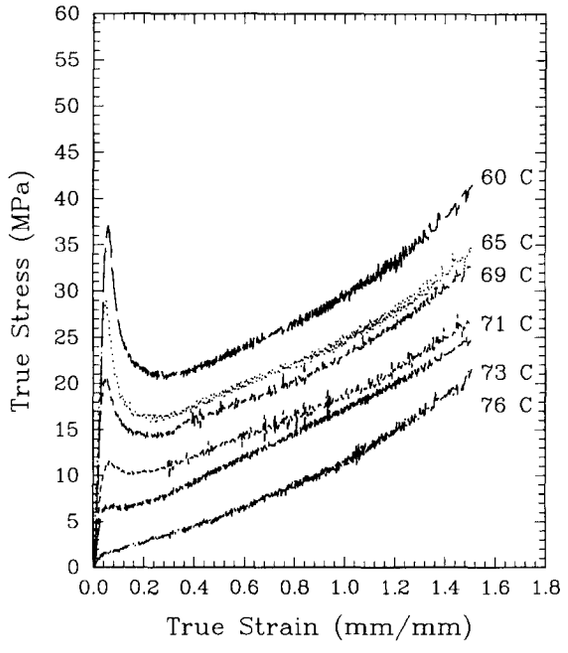

Figure 4 Isothermal uniaxial compression at 60–76°C and $-0.01\,s^{-1}$: effect of deformation temperature on mechanical properties in the glass transition region

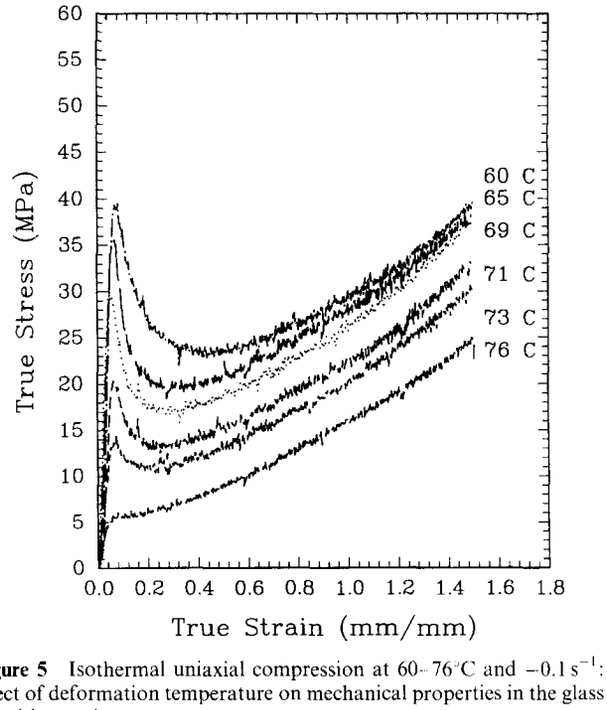

Figure 5 Isothermal uniaxial compression at 60–76°C and $-0.1\,s^{-1}$: effect of deformation temperature on mechanical properties in the glass transition region

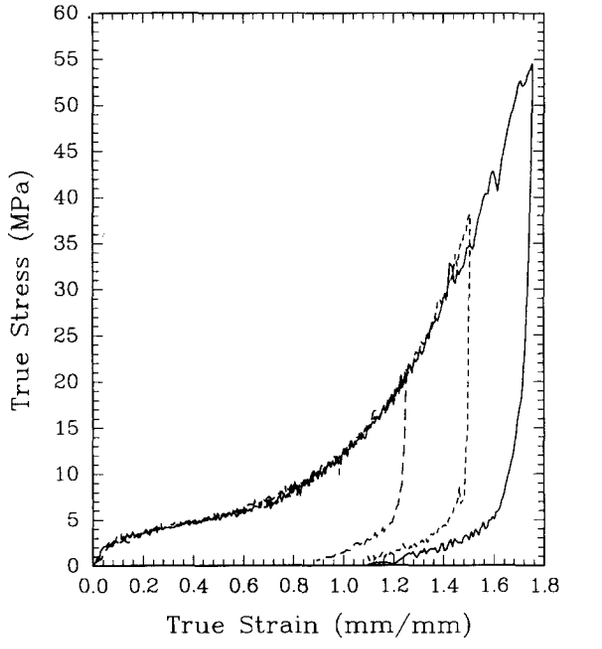

Figure 6 Adiabatic uniaxial compression at 80°C and $-0.5\,s^{-1}$: effect of deformation temperature on mechanical properties in the rubbery region

decreases more rapidly with increasing deformation temperature than the flow stress.

3. The height of the ageing peak (percent difference in peak stress vs flow stress), which was insensitive to experimental temperature up to 60°C, decrease at a rapid rate in the vicinity of T_g*. Strain softening from the yield to the flow stress occurs over the same level of true strain for both strain rates.
4. The strain hardening subsequent to yield is not sensitive to deformation temperature between 60°C and 76°C.

Figure 6 shows the adiabatic uniaxial compression in the rubbery region at 80°C at a strain rate of $-0.5\,s^{-1}$ to final imparted strains of −1.25, −1.5 and −1.75 respectively. PET flows without any apparent yielding under these conditions since the experimental temperature is above the glass transition; however, the strain hardening

* The fact that it is slightly higher for the 60°C data than for the 25°C and 50°C data could be attributed to the heating prior to testing in the thermal environment of the furnace resulting in some additional ageing; these effects are discussed in greater detail in the d.s.c. section.

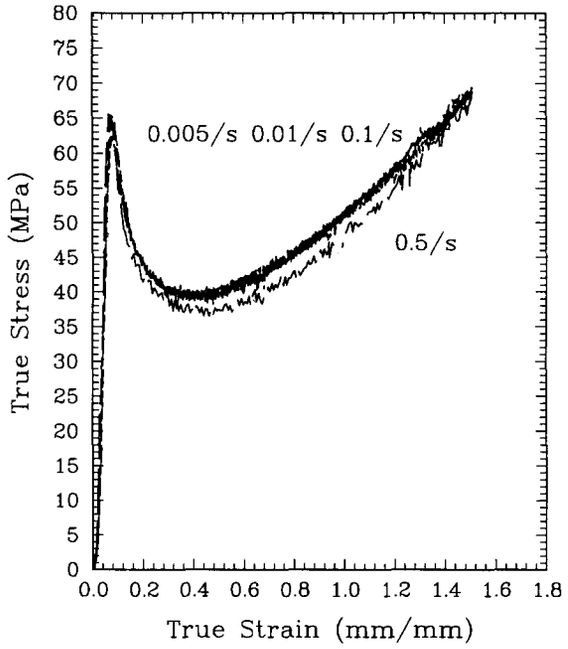

Figure 7 Uniaxial compression at 25°C and −0.005, −0.01, −0.1, $-0.5\,s^{-1}$: effect of heat transfer conditions on the flow stress

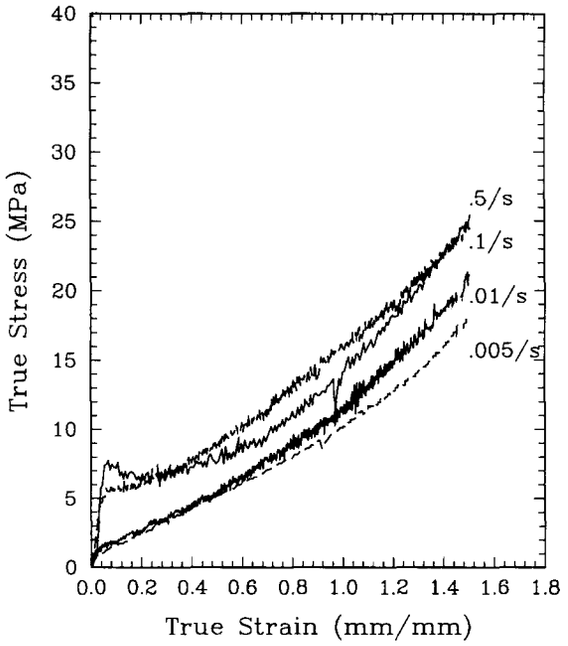

Figure 8 Uniaxial compression at 73°C and −0.005, −0.01, −0.1, $-0.5\,s^{-1}$: effect of strain rate on mechanical properties

modulus is much more pronounced than that observed in tests at temperatures between 60 and 76°C at the same deformation rate.

Effects of strain rate. *Figure 7* shows the uniaxial compression results at a temperature of 25°C, to a final true strain of −1.5 and strain rates −0.005, −0.01, −0.1 and $-0.5\,s^{-1}$. The tests for the three slowest rates exhibit nearly identical elastic plastic and subsequent strain hardening behaviour indicating low strain rate sensitivity at this temperature. However, the test at $-0.5\,s^{-1}$ that has been shown in the previous first order analysis to be adiabatic exhibits a lower flow stress.

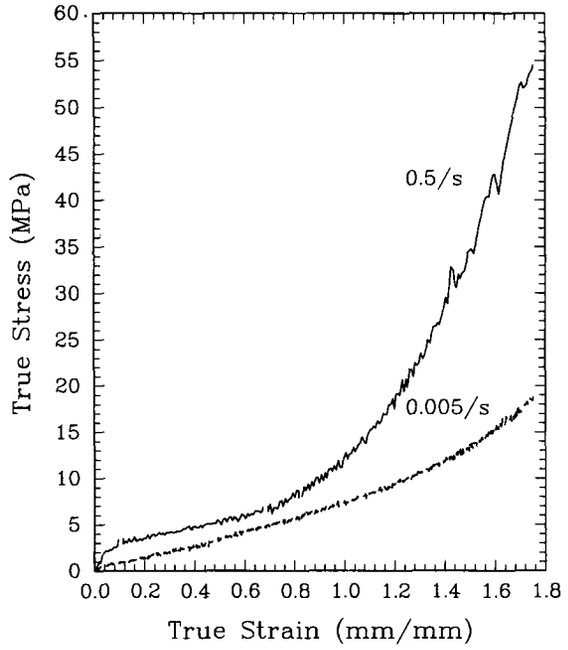

Figure 9 Uniaxial compression at 80°C and −0.005, $-0.5\,s^{-1}$: effect of strain rate on mechanical properties

The decrease in flow stress can be explained from the increase in temperature that results in the thermal softening of the material due to the adiabatic condition of the test. That effect leads to a lower apparent flow stress for the rapid test when compared to the slower strain rates. Hence the finding proves to be consistent with the first order analysis presented earlier*. *Figure 8* shows the uniaxial compression results at a temperature of 76°C to a final true strain of −1.5 and strain rates −0.005, −0.01, −0.1 and $-0.5\,s^{-1}$. The results show that the elastic modulus, yield and flow stress exhibit a pronounced sensitivity to strain rate in the T_g region.

An interesting behaviour is observed upon the deformation of PET in the rubbery regime. *Figure 9* shows the uniaxial compression at 80°C and strain rates of −0.005 and $-0.5\,s^{-1}$. In the rubbery regime the plasticity mechanism is inactive and hence the related phenomena, i.e. yield and strain softening, are absent. The distinctive difference between the rapid and slow rate occurs in the strain hardening behaviour: the $-0.5\,s^{-1}$ rate deformation exhibits a strain hardening behaviour that is much greater than that of the $-0.005\,s^{-1}$, suggesting the presence of strain-induced crystallization at $-0.5\,s^{-1}$. The hardening rate at $-0.005\,s^{-1}$ is lower than that observed in the 76°C data suggesting a molecular relaxation process dominating as temperatures get higher and strain rates lower. The result is consistent with the tensile stretching experimental observations of Jabarin *et al.*[14].

Figures 10–13 summarize the effects of temperature and strain rate on the mechanical behaviour in the glassy and glass transition region as they are reduced from the stress vs strain data. The variation of the elastic modulus with temperature and strain rate is shown in *Figure 10*. The variation clearly shows that the material is in the glassy region from 25 to 50°C and in the glass transition region from 60 to 76°C. It also shows that the rate of

* The apparent decrease in the flow stress is also observed in other polymers (see Arruda *et al.*[21])

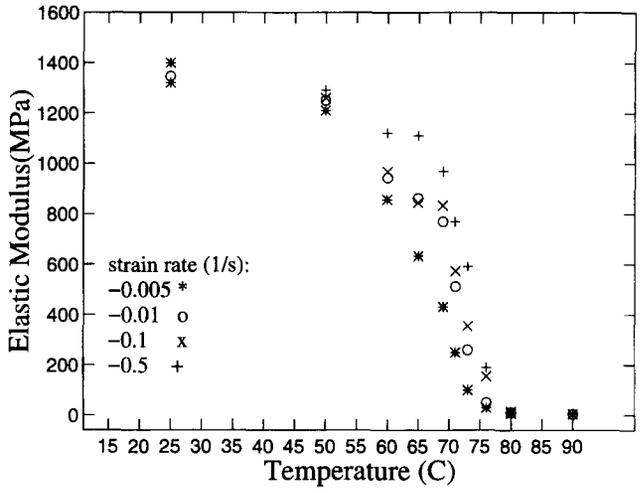

Figure 10 Compressive elastic modulus vs deformation temperature; uniaxial compression tests

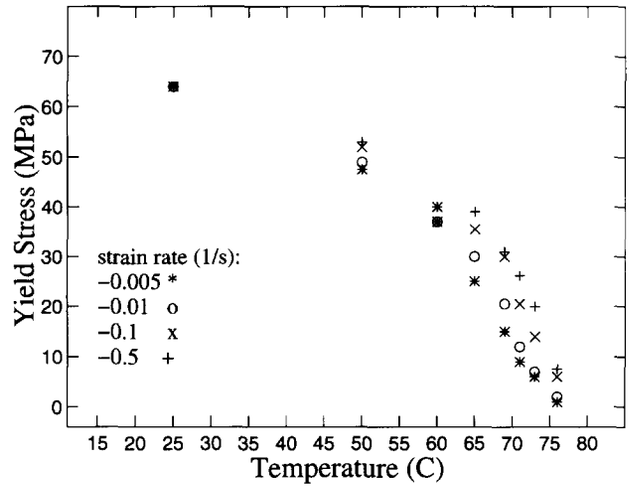

Figure 11 Compressive yield stress vs deformation temperature; uniaxial compression tests

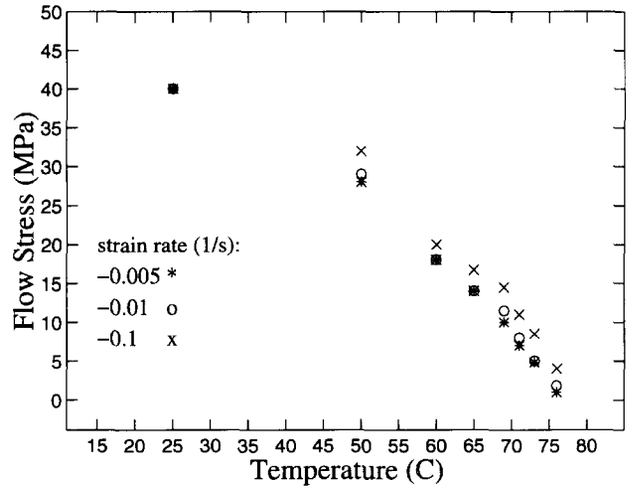

Figure 12 Compressive flow stress vs deformation temperature; uniaxial compression tests

deformation clearly affects the precise value of T_g as is well known: T_g increases with increasing strain rate. Furthermore, *Figures 11* and *12* show the decrease in yield and flow stress with increasing temperature and

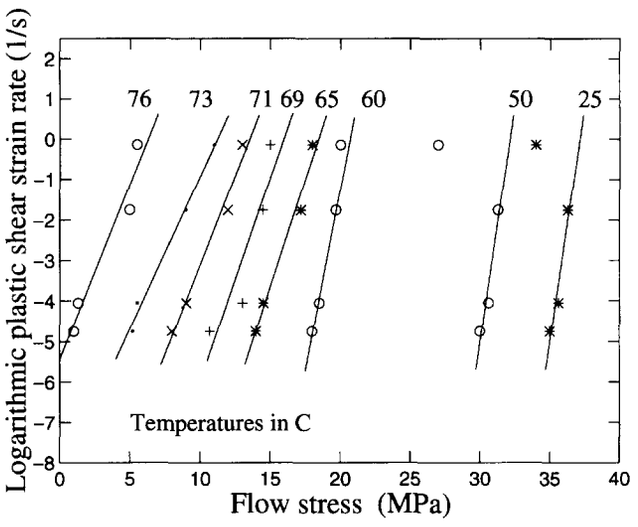

Figure 13 Eyring plot: variation of compressive flow stress vs logarithmic plastic strain rate; uniaxial compression tests

Table 3 Residual strain measured 48 h for the uniaxial compression to an imparted strain of −1.5 at 60–76°C and −0.005 to −0.5 s^{-1}

Temperature (°C)	−0.005 s^{-1}	−0.01 s^{-1}	−0.1 s^{-1}	−0.05 s^{-1}
60	1.26	1.21	1.16	1.18
76	0.79	0.56	0.79	0.67

decreasing strain rate. Note the nearly linear variation of the flow stress data with the natural logarithm of the plastic strain rate* as shown in *Figure 13*. This type of variation suggests the exponential dependence of the flow stress to the plastic strain rate over a wide range of temperatures in the glass transition regime, a finding which is consistent with data from other polymers. Finally, our data show that as the temperature increases the amount of recovery upon unloading increases. This is evident from the variation of the specimen residual strain with temperature (see *Table 3*) which demonstrates that uniaxial compression below T_g does not result in full recovery even at 76°C.

Effects of state of strain. Plane strain compression tests were performed at an isothermal constant strain rate of −0.01 s^{-1} in the same range of temperatures; results for the −0.01 s^{-1} rate and deformation temperatures of 60 to 76°C are presented in *Figure 14*. When compared to the uniaxial compression results, the latter results differ from the former in the initial yield, strain softening and the finite strain behaviour. Direct comparison can be seen in *Figure 15* for glassy and glass transition region behaviour respectively. Both figures show that the yield stress is slightly higher in plane strain compression than in the uniaxial compression tests. The trend can be explained partly from the apparent increase in yield stress due to the state of strain (if we employ the von Mises criterion) and partly from the hydrostatic

*The plastic shear strain rate $\dot{\gamma}_p$ is related to the experimental compression strain rate $\dot{\epsilon}_p$ by the von Mises relation: $\dot{\gamma}_p = \dot{\epsilon}_p\sqrt{3}$ and the flow stress σ is related to the shear flow stress τ by $\tau = \sigma/\sqrt{3}$

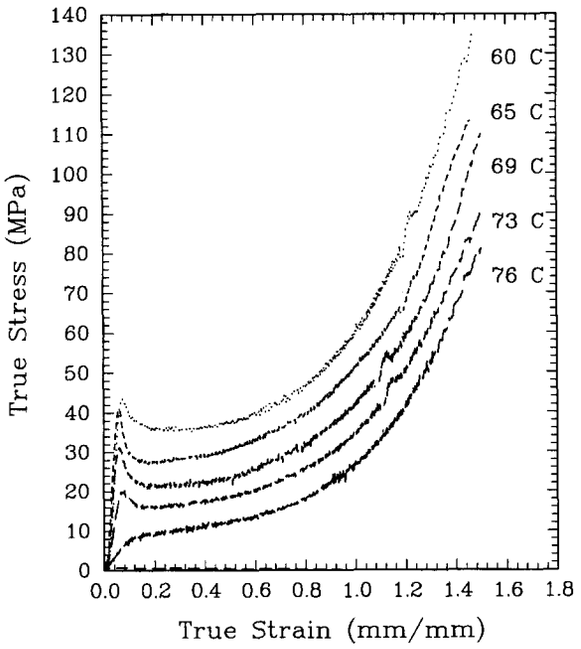

Figure 14 Isothermal plane strain compression at 60–76°C and $-0.01\,s^{-1}$: effect of deformation temperature on mechanical properties in the glass transition region

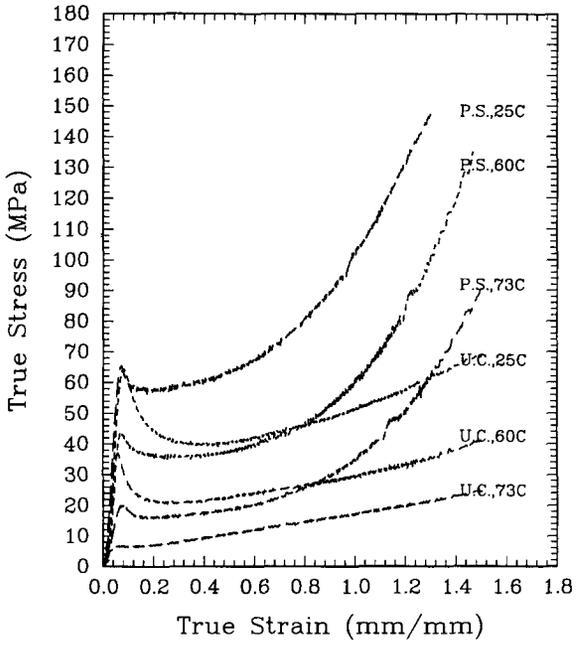

Figure 15 Comparison of plane strain and uniaxial compression behaviour at 25 and 60°C and $-0.01\,s^{-1}$

pressure effect on the yield stress*. The different strain hardening behaviour observed here under the two states of strain where the plane strain is much harder, has also been observed in PMMA and PC by Arruda *et al.*[20] where it was found that the difference can be attributed to the evolution in molecular orientation with state of strain for polymers which remain amorphous after deformation. In the case of PET, this difference in strain hardening may also be due to strain-induced crystallization. The effects of deformation on crystallization are evident from the d.s.c. measurements that follow.

* The pressure effect has been thorougly investigated by Ward *et al.*[11] who noted a pressure, p, dependence on the yield of PET of the order of $a = 0.175$ in $\tau = \tau_0 + ap$ if τ and τ_0 are the pressure modified and unmodified shear yield stresses respectively

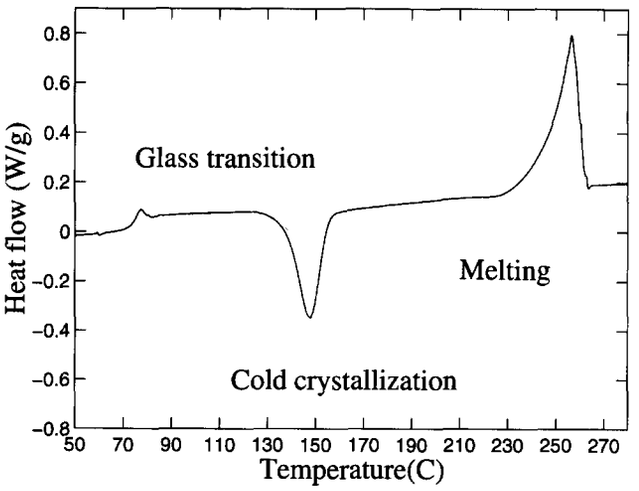

Figure 16 D.s.c. thermogram for the undeformed (as received) PET at a constant heating rate of $10°C\,min^{-1}$

Differential scanning calorimetry

D.s.c. scans were performed on samples in the as-received condition as well as samples which were deformed in uniaxial and plane strain compression to different levels of imparted strain at different temperatures and strain rates in their unloaded condition. The d.s.c. results enable the assessment of the percent crystallinity content through analysis of the cold crystallization behaviour.

Figure 16 shows a standard thermogram, i.e. the variation of heat flow into the sample as a function of increasing temperature, at a constant heating rate of $10°C\,min^{-1}$ on the as-received PET. At that particular heating rate, the T_g is observed at approximately 73.5°C. The observed value is consistent with our mechanical tests which show the rapid decrease in the yield and flow stress and the erasure of the ageing effect when the deformation (uniaxial/plane strain compression) temperature approaches 73 ± 1°C. The glass transition does not exhibit a smooth enthalpic transition indicating that the material has undergone physical ageing, where ageing manifests itself as the well known endothermic overshoot at T_g. Furthermore, as the temperature is increased beyond T_g the material begins to crystallize in the d.s.c. pan, where the onset of T_{cc} is observed at 137°C at this rate of heating and the area of cold crystallization (A_{cc}) is equal to $32\,J\,g^{-1}$. As the temperature is increased further, the crystals begin to melt at an approximate temperature of 239 ± 1°C. The melting of the crystals manifests itself as a wide endotherm whose peak is approximately at 252 ± 1°C and its area (A_m) is equal to $45\,J\,g^{-1}$.

Based on a two phase-(crystalline–amorphous) model, the weight percent crystallinity of the as-received material can be estimated. The weight percent crystallinity p_c is given as,

$$p_c = \frac{\Delta H_m - \Delta H_{cc}}{\Delta H_f} \qquad (2)$$

where ΔH_{cc} is the enthalpy released during cold crystallization, ΔH_m is the enthalpy required for melting and

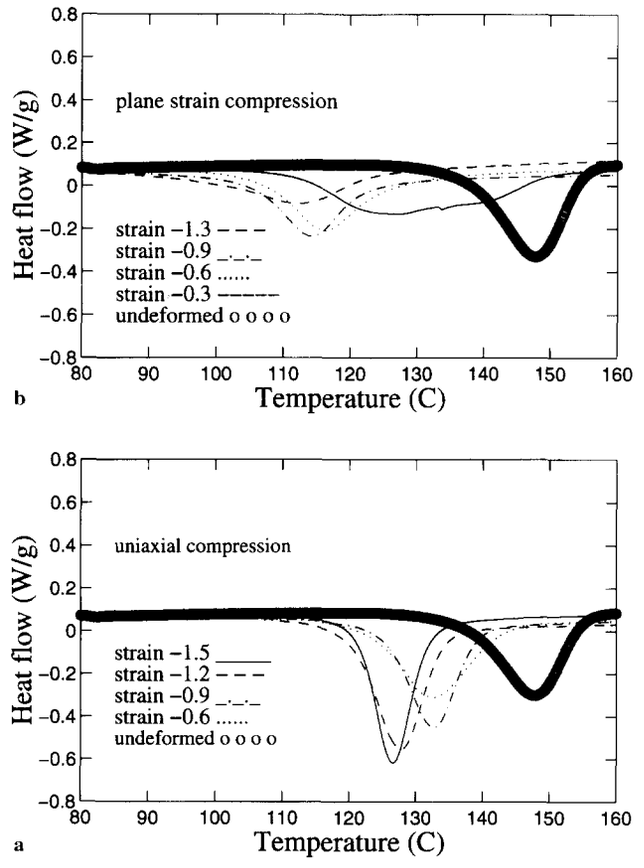

Figure 17 Cold crystallization behaviour as a function of imposed strain, uniaxial (a) plane strain compression (b), $-0.01\ s^{-1}$, 25°C

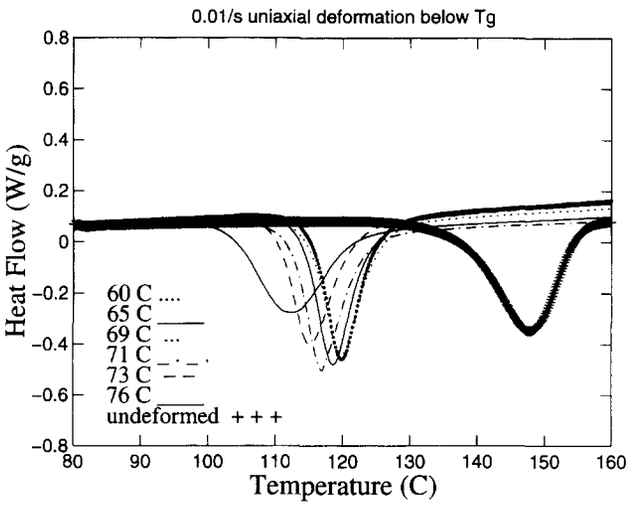

Figure 18 Cold crystallization behaviour as a function of deformation temperature, (60–76°C), uniaxial compression, $-0.01\ s^{-1}$

ΔH_f is the enthalpy of fusion of PET crystals, taken to be equal to $120\ J\ g^{-1}$*.

Equation (2) gives an initial crystallinity content for the received material of the order of 9%. It should be noted that this kind of quantitative analysis from d.s.c. data requires fully corrected data, i.e. elimination of residual enthalpy readings from the signal and appropriate choice of integration limits, since the accuracy of the method depends heavily on the measurement of the crystallization and melting areas with respect to the fully corrected baseline†. Furthermore, in order to ascertain the possible effects of the furnace thermal environment on the material prior to mechanical testing, we heated as-received PET at 65 and 75°C for 30 min and then cooled to room temperature in the furnace. The temperatures chosen are characteristic of the temperatures at which mechanical deformation was later imparted and the heating time chosen far exceeds the characteristic residence time of the sample in the furnace prior to and in the course of testing. For the two thermal treatments, the glass transition behaviour is slightly different, namely, the endothermic overshoot is pushed to a lower temperature. At the same time, the imposed thermal history does not change the onset temperature and energy magnitude of the cold crystallization exotherm, therefore indicating that heating the material to the desired test temperature maintains the amorphous structure of the sample.

Cold crystallization phenomena in the glassy, glass transition and rubbery region. Deformation is observed to impact the crystallization in the d.s.c. analysis. *Figure 17a* shows the effects of different levels of imparted strain on T_{cc} for samples strained in uniaxial compression at $-0.01\ s^{-1}$, 25°C. It can be seen that as the imparted strain increases, T_{cc} decreases markedly; a result most likely due to the orienting of the macromolecular network creating a more favourable structure for crystallization. Also, the area of the cold crystallization exotherm remains invariant to strain ($\approx 31\ J\ g^{-1}$) thus showing that the microstructure of the deformed and then unloaded samples is still amorphous. *Figure 17b* shows the effects on T_{cc} of the different levels of imparted strain at the same deformation rate and temperature for samples strained in plane strain compression. The more pronounced strain hardening of the plane strain condition (see *Figure 15*) can, in part, be attributed to stronger network orientation that in turn manifests itself as lower T_{cc} in the d.s.c. thermogram. However, not only are the onset temperatures of the exotherms lower in plane strain, but the cold crystallization area of the sample strained to −1.3 is now smaller than $\approx 32\ J\ g^{-1}$, about $\approx 21\ J\ g^{-1}$, indicating an increase in crystallinity content to 23%. It is not clear whether the crystallinity is concurrent with deformation or occurs immediately after; however, it appears that the amount of stretching is sufficient for macromolecules to lock in a stable crystalline configuration even when deformation is imparted at 25°C.

Figures 18 and *19* show the effects of imparted strain of the order of −1.5 applied at different deformation temperatures from 60 to 76°C at $-0.01\ s^{-1}$ and $-0.1\ s^{-1}$ strain rates respectively in uniaxial compression. Comparing the thermograms of the samples deformed under these conditions to that of undeformed PET we see that:

1. T_{cc} after an applied strain of −1.5 is significantly lower than that of the undeformed sample for all deformation temperatures. We also note T_{cc} decreases with deformation temperature and that the cold crystallization exotherm area may become more diffuse as the temperature at which strain was imparted increases.
2. The area of the crystallization exotherm is practically constant $\approx 32\ J\ g^{-1}$ for the uniaxial compression

* Personal communication with Dr D. P. Jones of ICI Films, UK
† There are several methods for the measurement of crystallinity such as n.m.r., X-ray, density, etc. For a comprehensive review of these methods see ref. 11. For other applications of the above method see refs. 5, 6 and 10

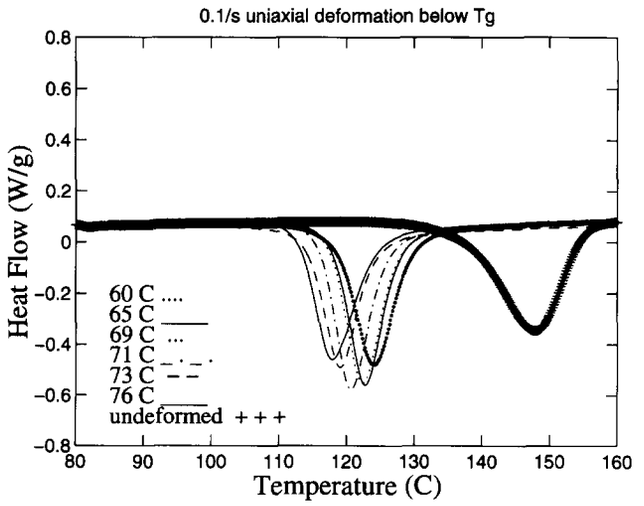

Figure 19 Cold crystallization behaviour as a function of deformation temperature (60–76°C), uniaxial compression, $-0.1\,s^{-1}$

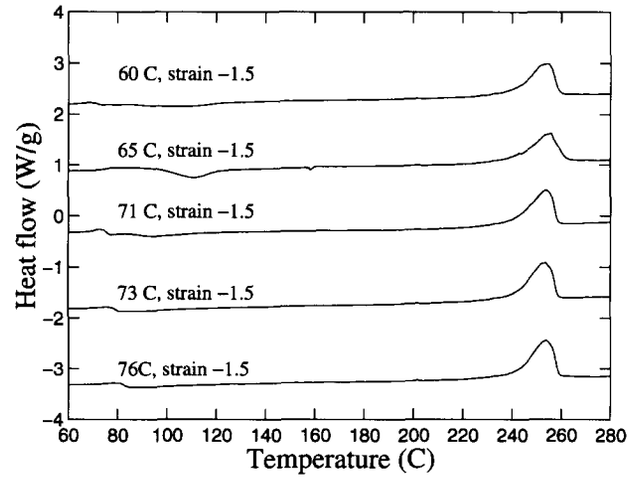

Figure 20 D.s.c. thermograms for samples deformed in plane strain compression in the temperature range 25–76°C and a strain rate of $-0.01\,s^{-1}$

temperatures considered (25–76°C). The areas of the corresponding melting endotherms, not shown here, are also constant as one would expect, where their onset is observed at $\approx 239 \pm 1$°C and their areas are constant and equal to $\approx 44\,J\,g^{-1}$. Our melting endotherm characteristics are consistent with the values reported by Guan *et al.*[6].

3. From equation (2) and the conditions examined above it follows that strain-induced crystallization is *absent* at temperatures below and in the glass transition region over the rates examined when the material is deformed in uniaxial compression.
4. As deformation temperature increases, the onset of the cold crystallization exotherm decreases. However, no marked difference in strain hardening was observed for the mechanical tests over the range of deformation temperatures.

The results of the d.s.c. scans on the samples deformed in plane strain compression in the same temperature range of 60 to 76°C and at a strain rate of $-0.01\,s^{-1}$ are shown in *Figure 20*. The following trends should be noted:

1. T_{cc} after an applied strain of -1.5 is significantly lower than that of the undeformed sample for all deformation temperatures as well as the T_{cc} values of samples deformed in uniaxial compression under the same deformation conditions. Owing to the very diffuse nature of the cold crystallization phenomenon and its proximity to T_g, it is very difficult to measure exact values for T_{cc} and A_{cc} (≈ 0).
2. The areas of the corresponding melting endotherms do not change considerably with deformation temperature: Their onset is observed at $\approx 241 \pm 1$°C and their areas are constant and equal to $\approx 52\,J\,g^{-1}$. Onset and peak values are the same as in the uniaxial compression, however, the areas of the melting peaks are significantly higher in plane strain than in uniaxial compression.
3. From equation (2) and the conditions examined above, it follows that crystallization is present at temperatures below and in the glass transition region over the rates examined when the material is tested in plane strain compression. The end crystallinity for the samples tested in plane strain compression is of the order of 41%.

The plane strain d.s.c. results show considerable increase in crystallinity with imparted strain at deformation temperatures ranging from 25 to 76°C. However, as deformation temperature increases, the effect of heat setting the strained amorphous phase in the plane strain fixture becomes a possibility. Separating the crystallization contribution of heat setting and strain is not possible from the d.s.c. readings since crystallinity was measured on the sample after cooling.

Furthermore, the effects of temperature, strain rate and imparted uniaxial strain on T_{cc} are equally interesting when the material is tested in the rubbery region: the microstructural state of the samples deformed to final strains of -1.25, -1.5, -1.75, at $-0.5\,s^{-1}$ and 80°C are shown in *Figure 21a*: consistent with *Figures 17a, b*, T_{cc} is depressed as the imparted strain increases. Unlike the uniaxial compression tests below the glass transition, however, as imparted uniaxial strain increases, the area of the cold crystallization exotherm decreases. It can be inferred that strain induced crystallization evolves in the material during uniaxial compression. The end crystallization of the sample strained to a final uniaxial strain of -1.75 is of the order of 18%. *Figure 21b* shows the thermograms of samples deformed to final strains of -1.5, -1.75, at $-0.005\,s^{-1}$ and 80°C. The depression of T_{cc} is significant, indicating network orientation due to the deformation, and the depression of A_{cc} indicates strain-induced crystallization. The end crystallization of the samples strained to final strains of -1.5 and -1.75 are of 15% and 19% respectively.

DISCUSSION AND CONCLUSIONS

Both the mechanical tests and the post deformation microstructural analysis show that the mechanical behaviour of PET is a strong function of deformation temperature.

- For a fixed deformation temperature, as the imparted strain increases the material deforms elastically then yields and eventually strain hardens. As the deformation temperature increases and the strain rate decreases, the elastic modulus, yield stress and flow stress decrease

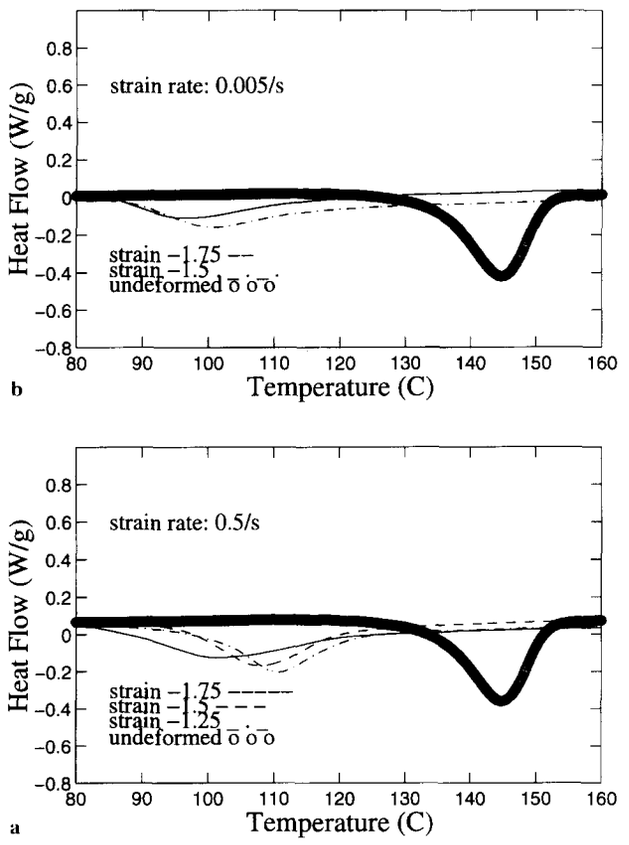

Figure 21 Cold crystallization behaviour as a function of imparted true strain (0 to −1.75), uniaxial compression, 80°C. (a) $-0.5\,s^{-1}$, (b) $-0.005\,s^{-1}$

to the point where ageing effects vanish when the deformation temperature is just above T_g. Uniaxial compression tests show the linear dependence of the flow stress to the logarithm of the plastic strain rate. This linear dependence suggests the modelling of the flow process with a diminishing energy barrier thermal activation law.

- The uniaxial compression tests over a wide range of temperatures below and through the glass transition and a wide range of slow to rapid strain rates have shown that deformation of the order of −1.5 in true strain does *not* result in strain-induced crystallization. This is evidenced by an essentially temperature invariant cold crystallization exotherm area. The evolution of the microstructure, was also monitored as a function of imparted strain. At a moderate isothermal strain rate $-0.01\,s^{-1}$ and 25°C deformation temperature, the macromolecular orientation becomes more pronounced as the imparted strain increases (demonstrated by the depression of T_{cc}), while the cold crystallization area remained constant indicating no strain-induced crystallization.
- The same trends in mechanical behaviour are observed in the results of the plane strain compression tests. The strain hardening behaviour is moderately depressed as deformation temperature approaches the glass transition; however, consistent with the behaviour observed in other amorphous polymers, it is always much greater than that observed in the uniaxial compression. The more severe strain hardening observed in plane strain compression than in uniaxial is, at least in part, the result of more severe macromolecular orientation. Indeed, the $-0.01\,s^{-1}$, 25°C deformations at various levels of imparted strain show a higher depression of T_{cc}, with imparted strain than in uniaxial compression hence validating the above hypothesis. At the same time however, A_{cc} is depressed considerably with imparted strain which shows that strain-induced crystallization occurs in plane strain compression even at 25°C. The strain-induced crystallization may also contribute to the higher hardening rate. Furthermore, a high value of end crystallinity (41%) of samples deformed in plane strain at $-0.01\,s^{-1}$ tested from 60 to 76°C indicates that in plane strain below T_g the polymer deforms as an amorphous structure that crystallizes in the plane strain fixture either during or after the course of deformation. Thus, precise material structure evolution during plane strain compression cannot be quantitatively assessed from subsequent d.s.c. analysis on the deformed specimens since there may be a post-stretch annealing effect. However, some crystallization was observed at 25°C where no annealing occurred.
- The mechanical behaviour of the material above T_g at 80°C is characterized by the extreme sensitivity of the strain hardening behaviour to strain rate. Rapid strain rates favour orientation and possible strain-induced crystallization manifested as pronounced strain hardening; whereas, very slow rates favour relaxation phenomena manifested as weak strain hardening. The extreme sensitivity of the material to the deformation conditions in the rubbery region impedes accurate control of the imparted deformations resulting in experimental results of low repeatability. Strain-induced crystallization estimates are difficult to obtain in that temperature region. The material can crystallize rapidly in the mechanical test upon unloading due to temperature and time; that additional crystallinity is measured in the d.s.c. thermogram in that way impeding the correlation of the temperature and strain rate sensitive strain hardening to developing crystallinity.

The similarity of the mechanical behaviour of PET in the transition to that of strictly amorphous polymers motivates the modelling of the above deformations in the transition region with a modified Arruda and Boyce constitutive model[20]. The phenomenological basis, mathematical formulation of the model as well as the results are provided in Zaroulis[24] and will be reported on in a separate paper.

ACKNOWLEDGEMENTS

The research has been funded by the NSF through grant number MSS-9215805 and, in part, through a PYI award to MCB (DMI-9157899) with matching funds from Du Pont. The Perkin Elmer DSC-7A equipment was made available through the NSF funded MIT Center for Materials Science and Engineering (DMR-9400334). The PET film was supplied by D. P. Jones of ICI Films, UK.

REFERENCES

1 Marshall, I. and Thompson, A. B. *J. Appl. Chem.* 1954, **4**, 145
2 Marshall, I. and Thompson, A. B. *Proc. Roy. Soc. of Lond.* 1954, **A221**, 541
3 Thompson, A. B. *J. Polym. Sci.* 1959, **34**, 741

4 Ward, I. M. *J. Macromol. Sci.* 1967, **4**, 667
5 Ghanem, A. M. and Porter, R. S. *J. Polym. Sci. Part B: Polym. Phys.* 1989, **27**, 2587
6 Guan, J. Y., Wang, L. and Porter, R. S. *J. Polym. Sci. Part B: Polym. Phys.* 1992, **30**, 687
7 Sun, T., Pereira, J. and Porter, R. S. *J. Polym. Sci. Polym. Phys. Edn* 1984, **22**, 1163
8 Misra, A. and Strein, R. S. *J. Polym. Sci. Polym. Phys. Edn* 1979, **17**, 235
9 Buckley, C. P., Jones, D. C. and Jones, D. P. *Polymer* 1996, **37**, 2403
10 Blundell, D. J., Beckett, D. R. and Willcocks, P. H. *Polymer* 1981, **22**, 704
11 Kavesh, S. and Schultz, J. M. *Polym. Eng. Sci.* 1969, **9**, 331
12 Ward, I. M., Rabinowitz, S. and Duckett, A. *J. Mater. Sci.* 1970, **5**, 29
13 Jabarin, S. A. *Polym. Eng. Sci.* 1992, **32**, 1341
14 Jabarin, S. A. and Chandran, P. *Adv. Polym. Tech.* 1993, **12**, 119
15 Arruda, E. M. and Boyce, M. C. *Polym. Eng. Sci.* 1990, **30**, 20
16 Arruda, E. M. and Boyce, M. C. *Int. J. Plasticity* 1993, **9**, 697
17 Imai, M., Mori, K., Mizukami, T., Kaji, K. and Kanaya, T. *Polymer* 1992, **33**, 4457
18 Hasan, O. A. and Boyce, M. C. *Polym. Eng. Sci.* 1995, **35**, 331
19 Boyce, M. C., Parks, D. M. and Argon, A. S. *Mechanics of Materials* 1988, **7**, 15
20 Arruda, E., Boyce, M. C. and Jachandran, R. *Mechanics of Materials* 1995, **19**, 193
21 Brandrup, J. and Immergut, E. H. (eds) 'Polymer Handbook', 3rd Edition, New York, Wiley, New York, 1989
22 Hasan, O. A. and Boyce, M. C. *Polymer* 1993, **24**, 1207
23 Hasan, O. A., Boyce, M. C., Li, X.S. and Berko, S. *J. Polym. Sci. Part B: Polym. Phys.* 1993, **31**, 185
24 Zaroulis, J. S. S.M. Thesis, Department of Mechanical Engineering, Massachusetts Institute of Technology, 1995